

**Detecting generalized synchrony: An improved approach**Daihui He,<sup>1,2</sup> Zhigang Zheng,<sup>3,4</sup> and Lewi Stone<sup>1,\*</sup><sup>1</sup>*Biomathematics Unit, Tel Aviv University, Ramat Aviv, Tel Aviv 69978, Israel*<sup>2</sup>*Department of Mathematics and Statistics, McMaster University, Hamilton L8S 4K1, Canada*<sup>3</sup>*Department of Physics, California Institute of Technology, Pasadena, California 91125*<sup>4</sup>*Department of Physics, Beijing Normal University, Beijing 100875, China*

(Received 2 September 2002; published 27 February 2003)

We examine some of the difficulties involved in detecting generalized synchrony (GS) in systems that exhibit noninvertibility and/or wrinkling. These latter features severely hinder identification of GS by conventional techniques. It is shown that it is possible to greatly improve detection by reducing the pseudofalse neighbors effects. Here we propose the  $\delta^p$ -neighbor method to overcome the noninvertibility effect and the  $\delta^{p,q}$  method to detect GS in systems with wrinkled structures.

DOI: 10.1103/PhysRevE.67.026223

PACS number(s): 05.45.-a, 87.10.+e, 87.19.La

**I. INTRODUCTION**

The synchronization of coupled and driven chaotic systems embeds order in the presence of otherwise very complex dynamics [1]. Various types of chaotic synchronizations such as identical synchronization, generalized synchronization (GS), and phase synchronization have been described recently. Generalized synchronization is characterized by the existence of a continuous map  $\phi: X \rightarrow Y$  between the phase spaces  $X$  and  $Y$  of a drive and a response system. GS has a variety of applications in physical and biological systems [2], where the detection of GS (and other types of synchrony) is an important issue. However, the detection processes depend crucially on the underlying specific systems and can be influenced by numerous factors. Among these, typical complications such as *noninvertibility* and *wrinkling* in models that exhibit GS have recently attracted much attention [3–6] from both theoretical and experimental viewpoints. Noninvertibility, which makes the function  $\phi$  multivalued and the synchronization set smeared, generally, is a very important feature in biological population dynamics and neuronal system with time delays [3,4]. For invertible systems, the synchronization set can become nondifferentiable by wrinkling, which makes it difficult or even impossible to obtain useful information of the drive system from observations of the response system [5,6]. In terms of experimental systems, both wrinkled and smeared synchronization sets have been observed in coupled electronic circuits [3,7].

Recently, the authors of Ref. [3] studied the effect of wrinkling and smearing on the detection of nonlinear synchrony [3]. They pointed out that most GS detection methods are based on measuring the continuity of  $\phi$ , as follows: For a coupled drive-response system, after transients die out, one may pick a point  $(X, Y)$  on the attractor and a ball  $B[X, \delta]$  of small radius  $\delta$  about this point. Integrate the full system until the  $X$  component of the trajectory lands in the ball  $B[X, \delta]$  a large number of times and keep a record of these  $\delta$  neighbors. Denote by  $\varepsilon_{max}$  the largest distance between their corresponding  $Y$  components. When  $\varepsilon_{max} \rightarrow 0$  linearly as  $\delta$

$\rightarrow 0$ , the authors of Ref. [3] argue that the response system is in a continuous functional relationship with the drive, and the systems exhibit GS. They found that due to noninvertibility, smearing and wrinkling, this linear relationship often breaks up, making the experimental detection of synchrony (GS in their work) by this method difficult if not impossible.

Detection of GS in experimental work usually takes advantage of the idea of mutual false nearest neighbors [8]. The reconstruction of the embedding phase space  $R_E$  from a scalar variable  $r(t)$  of the response system and the embedding phase space  $D_E$  from a scalar variable  $d(t)$  taken from the drive system has been described in Ref. [8]. Careful reconstruction, with attention to embedding dimension [9], is necessary to define the suitable nearest neighbors in practical applications. Furthermore, the effect of *pseudofalse* neighbor points must be taken into account [10]. The pseudofalse neighbor points are true neighbor points in the reconstructed attractor, while they are considered to be unsuitable when local methods are adopted to predict chaotic time series. However, as we discuss in detail below, the local prediction used in Ref. [3] neither uses appropriate embedding nor takes into consideration the effect of pseudofalse neighbors when trying to detect GS. In this paper, we adapt the  $\delta$ -neighbor method (e.g., appropriate embedding dimension, removal of pseudofalse neighbors), and find that in contrast to the analysis of Ref. [3], a linear  $\varepsilon_{max}$ - $\delta$  relationship can be found for GS, even in systems that wrinkle or are noninvertible. This study implies the feasibility of experimental detection of GS in practice.

**II. THE PSEUDOFALSE NEIGHBOR METHOD**

In our view, it might be possible to detect GS by the methods of Ref. [3] if time series embedding is used and the effect of pseudofalse neighbors is removed. Consider, for instance, the drive system of the first (wrinkled) example in Ref. [3]—the generalized Baker's map. The attractor of the drive has the box-counting dimension  $D_0 = 2$ . The difficulties of detecting GS, as described in Ref. [3] arise because they fail to take into account this dimensionality. Embedding the data in the spirit of Takens embedding theorem [11] proves to be useful here. In this respect, we make use of the

\*Author to whom correspondence should be addressed.

“ $\delta^p$  neighbor” approach, as described in Ref. [10], which attempts to reduce the influence of the pseudofalse neighbor points by carefully tracking the trajectory, its nearest neighbors and their preimages after the data has been embedded.

The definition of  $\delta^p$  is as follows [10]: In the reconstructed state space, for a particular reference point  $X_N$ , where  $N$  is the time index, the  $k$  “usual”  $\delta$ -neighbor points of  $X_N$  are notated as  $X_{N(j)}$ ,  $j=1,2,\dots,k$ . These neighbors satisfy the condition  $\|X_{N(j)} - X_N\| < \delta$ , where  $\|\cdot\|$  represents Euclidean distance. The  $\delta^p$ -neighbor points take into account the  $p$  preimages as well. The neighbors  $X_{N(j,p)}$ ,  $j=1,2,\dots,k$  are defined as those points satisfying  $\|X_{N(j)-i} - X_{N-1}\| < \delta$  for every  $j$  and  $0 \leq i \leq p$ . The approach thus uses previous segments or pattern found in the drive or response data to enhance the prediction. (Note that strictly speaking, this method of preimages is not completely equivalent to Taken’s scheme for phase space reconstruction.) The main rationale behind this strategy [10] is that the  $\delta^p$ -neighbor points lie near the reference point not only in state space, but also in tangent space. Similar ideas have been used to identify the embedding dimension [10–12], where the directions of vectors in a neighborhood are examined to exclude the false crossing caused by an improperly reconstructed space. It is necessary and reasonable to introduce the  $\delta^p$  neighbor to the detection of GS, especially for noninvertible systems. Due to the noninvertibility, a typical state of the drive will have a whole tree of possible histories, and recurrences in the drive may thus occur along different routes. Each such route provides a different driving signal. Therefore, for almost all points in the drive there typically corresponds a Cantor set of points in the response: one for each drive history [3]. The  $\delta$  neighbor used in Ref. [3] is in fact the special case of the  $\delta^p$  neighbor with  $p=0$ . Therefore, it is hardly surprising that the  $\delta^0$  neighbors includes a large percent of pseudofalse neighbors, and the prediction, of course, is much worse when wrinkling and noninvertibility is present. A direct way to improve the prediction is to increase the number of preimages  $p$ .

With regard to the experimental detection of GS, in most cases the drive and response signals are measured as scalar data. Similar to the  $\varepsilon_{max}$ - $\delta$  scheme, a reference point and its  $\delta^p$  neighbors are taken from the scalar signal of the drive. Their correspondences in the response system gives the  $\varepsilon_{max}$ . If there exists a GS between drive and response system, one may typically expect that  $\varepsilon_{max} \rightarrow 0$  linearly as  $\delta \rightarrow 0$ . This description includes the cases both  $p=0$  and  $p > 0$ . It can be found that with the pseudofalse neighbor approach, i.e.,  $p > 0$ , one may get a much better detection of GS than the unembedded case  $p=0$ . This scheme can be illustrated by examples adopted in Ref. [3]. Consider, for example, the noninvertible case discussed in Ref. [3] which is their “worst-case” situation where the ability to predict the state of the response system from the drive is severely limited. Unlike their results, we find that after taking  $p \geq 5$ , the  $\varepsilon_{max}$ - $\delta$  relation is extremely close to linear. In practice, the use of a segment  $p > 0$  rather than an instantaneous state  $p=0$ , enhances prediction of consequent states. This is because with noninvertible systems,  $\delta^0$  neighbors often have

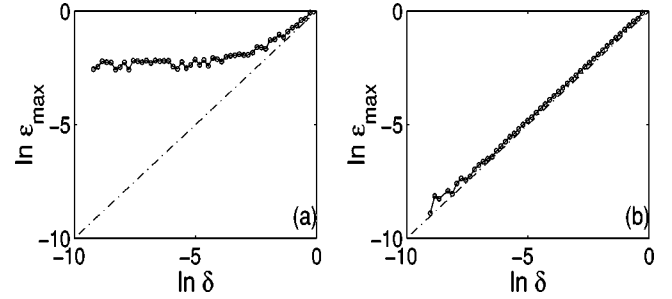


FIG. 1. Simulation result of the two-dimensional piecewisely linear map (1): (a) result of Ref. [3]; (b) our result by using the  $\delta^p$ -neighborhood prediction with  $p=7$ . The dot-dashed line is the theoretically expected linear relation.

very different historic trajectories (preimages), and cannot be used as a guide for local prediction. The  $\delta^p$  neighbors, on the other hand, all have similar histories and corresponding states in the response system can be used as a guide to predict consequent states. The choice of  $p$  should reflect the dimension of the attractor of the drive and response systems. In this paper, we chose 6–12 for one- and two-dimensional map systems, which was usually found to be sufficient.

For the case of wrinkling, we suggest using what we term  $\delta^{p,q}$  neighbors. Let  $X_N$  and  $Y_N$  denote the original (or reconstructed) state of the drive and the response systems, respectively. The  $\delta^{p,q}$ -neighbor points  $X_{N(j,p,q)}$  ( $j=1,2,\dots,k$ ) are defined as those points satisfying  $\|X_{N(j)-i} - X_{N-1}\| < \delta$  for every  $j$  and  $0 \leq i \leq p$  and at the same time the corresponding state  $\|Y_{N(j)-l} - Y_{N-1}\| < \delta$  for every  $0 < l \leq q$ . The necessity for embedding the response systems (through  $q$ -dimensional neighboring system) as well as the drive is most likely due to the complex fractal structure of the synchronization set associated with wrinkled systems.

Just as with the  $\delta^p$ -neighbor method, we denote  $\varepsilon_{max}$  as the maximum value among all neighbors  $\|Y_{N(j)} - Y_N\|$ . For the above three definitions [ $\delta$ -,  $\delta^p$ -, and  $\delta^{p,q}$ -neighbor approaches], if  $\varepsilon_{max} \rightarrow 0$  linearly as  $\delta \rightarrow 0$ , then GS occurs between  $X_N$  and  $Y_N$ .

### III. RESULTS AND DISCUSSION

Below we illustrate the above approaches by investigating the following three models. These models are very typical noninvertible and/or smeared examples which have been studied in [3–6]. Reconstruction before reducing the pseudofalse neighbors is not necessary in these examples, because their original dimensions are very low (1 or 2). In this situation, the result of the original coordinates is similar with that of the reconstructed coordinates.

(a) *Two-dimensional piecewisely linear map.* This map is a *noninvertible* example and has been discussed in Ref. [3] to illustrate how noninvertibility hampers the detection of synchronization. The model is

$$x_{n+1} = \begin{cases} 2x_n, & x_n < 0.5 \\ 2(x_n - 0.5), & x_n \geq 0.5 \end{cases}$$

$$y_{n+1} = cy_n + x_{n+1}. \quad (1)$$

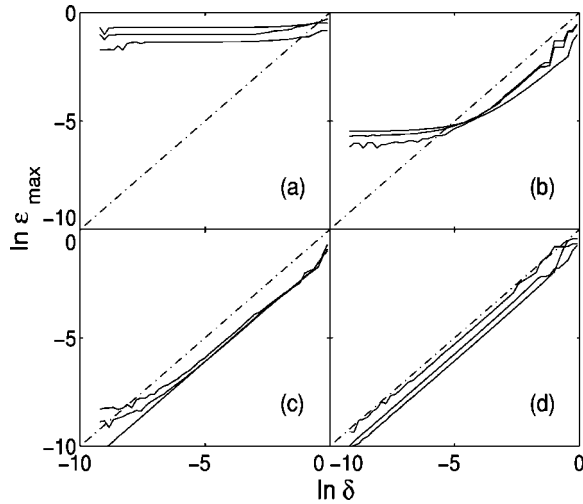


FIG. 2. Simulation results for the tent-map-driven logistic map (2). The  $\delta^p$ -neighborhood prediction with  $p=8$ . (a)  $\epsilon=0.2$ , (b)  $\epsilon=0.3$ , (c)  $\epsilon=0.4$ , and (d)  $\epsilon=0.5$ . The dash-dotted line gives the theoretical expectancy.

For  $|c| < 1$  the synchronization set is asymptotically stable. Here we use  $c=0.35$ , there is GS between  $x$  and  $y$ . In Fig. 1(a), the relation between  $\epsilon_{max}$  and  $\delta$  is numerically determined by using the  $\delta$ -neighbor approach, and the theoretically predicted linear line is plotted for purpose of comparison. It is found that  $\epsilon_{max}$  decreases with  $\delta$  far too slowly, indicating the poor detection efficiency of the  $\delta$ -neighbor approach. However, with the  $\delta^p$ -neighbors approach (with  $p \geq 5$ , for example,  $p=7$  here), Fig. 1(b) shows that  $\epsilon_{max}$  decreases linearly as  $\delta$ , implying the presence of GS between response and drive system. This indicates that the  $\delta^p$ -neighbor method detects GS in this noninvertible system while the  $\delta$ -neighbor method fails.

(b) *The tent-map-driven logistic map.*

$$x_{n+1} = \begin{cases} x_n/b, & x_n < b \\ (x_n - 1)/(b - 1), & x_n \geq b \end{cases}$$

$$y_{n+1} = (1 - \epsilon)ay_n(1 - y_n) + \epsilon x_{n+1}, \quad (2)$$

where the parameter  $b \in (0, 1)$  controls the symmetry of the tent map,  $a$  is the control parameter of the logistic map, and  $\epsilon$  is a coupling parameter. Here we use  $b=0.677$  and  $a=3.7$ . This drive-response map is also studied as a typical noninvertible case by Afraimovich *et al.* [4]. In Fig. 2, we fix  $p=8$  and vary  $\epsilon$  from 0.2 to 0.5. For each  $\epsilon$  three simulations are given beginning from different randomly chosen initial conditions. For the case  $\epsilon=0.2$ , where there is no GS [4] there is also no linear relation between  $\epsilon_{max}$  and  $\delta$ , as might be expected, no matter how large  $p$  [see Fig. 2(a)]. The diagonal linear relation becomes more apparent for larger  $\epsilon$  as seen in Figs. 2(b)–2(d). For the case  $\epsilon=0.6$ , which according to detailed analysis in Ref. [4] is synchronized, the  $\delta$ - $\epsilon_{max}$  curve is very close to linearity [same as  $\epsilon=0.5$  in Fig. 2(d)]. Thus using  $\delta^p$  neighbor with a suitable  $p$ , GS can be detected even when the relation is noninvertible. Generally for larger  $p$ , the prediction error is smaller. On the other

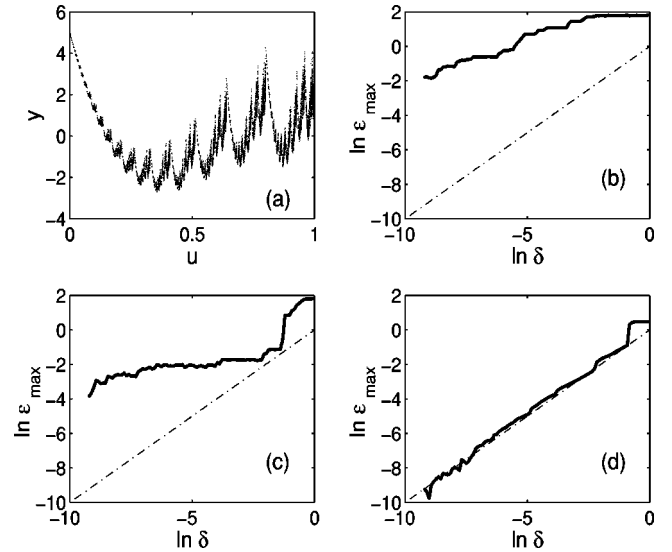


FIG. 3. Simulation result of the generalized Baker's map. (a) Complicated structures of the synchronization set. (b) Relation using the method given in Ref. [3]. (c) Relation using the  $\delta^p$ -neighborhood prediction  $p=12$ ; (d) relation using the  $\delta^{p,q}$ -neighborhood prediction  $p=4$  and  $q=1$ . In (b)–(d) the dotted line gives the theoretically expected result.

hand, a high  $p$  requires a larger quantity of raw data ( $N=10^6$  for Fig. 2), which would sometimes make the test procedure difficult for experimental applications.

(c) *The generalized Baker's map.* Wrinkling appears to make GS more difficult to detect than noninvertibility. For the latter, it is already clear that if the history of the drive is considered, a smoothlike relation can be found between response and drive signal [4]. To our knowledge, in the presence of wrinkling there is no such relationship. The mechanism of wrinkling has been exhaustively studied very recently [3,5,6]. In our view, the wrinkled attractor has properties that resemble that of a strange nonchaotic attractor, i.e., fractal structure with a negative Lyapunov exponent [13]. For the wrinkling case, increasing  $p$  helps little in detecting GS when we use the above method. However, the  $\delta^{p,q}$  approach, which includes both the history of the drive and the response when choosing suitable neighbors, provides a better diagonal relation between  $\delta$  and  $\epsilon_{max}$ . We illustrate the  $\delta^{p,q}$  approach with the following system [3,5,6]:

$$u_{n+1} = \begin{cases} \lambda u_n, & v_n < \alpha \\ \lambda + (1 - \lambda)u_n, & v_n \geq \alpha \end{cases}$$

$$v_{n+1} = \begin{cases} v_n/\alpha, & v_n < \alpha \\ (v_n - \alpha)/(1 - \alpha), & v_n \geq \alpha \end{cases}$$

$$y_{n+1} = cy_n + \cos(2\pi u_{n+1}). \quad (3)$$

Here  $\lambda \in (0, 1)$ ,  $\alpha \in (0, 1)$ . The Baker's map is iterated in a two-dimensional unit square. It has been shown that for  $|c| < 1$ , the response is asymptotically stable for all  $(u, v)$ . The synchronization set is typically nondifferentiable if the average contraction within the drive is larger than the contraction

in the response, and the development of this nondifferentiability is called wrinkling [3,5,6]. We chose the parameters as  $\lambda=0.8$ ,  $\alpha=0.7$ , and  $c=0.8$  following Refs. [3,5].

In Fig. 3(a), the complicated structure of the synchronization set is plotted. It can be seen that almost everywhere on the  $u$  axis, a randomly chosen  $u$  corresponds to a vertical segment of  $y$ . In Fig. 3(b), the  $\delta$ - $\varepsilon_{max}$  relation is plotted, as found by the  $\delta$ -neighbor method adopted in Ref. [3] (corresponding to the case  $p=0$ ,  $q=0$ ). The same relation by applying the  $\delta^p$ - $\varepsilon_{max}$  neighbor prediction with a very large  $p=12$  ( $q=0$ ) is plotted. Both curves deviate far from the linear relation, indicating difficulty in detecting GS. (Note that for the above chosen parameters the system actually achieves GS.) This implies that  $p$  alone cannot give a good prediction. In Fig. 3(d) we use the  $\delta^{p,q}$ -neighborhood prediction to detect GS with relatively small parameters  $(p,q)=(4,1)$ . The scaling relation coincides well with the theoretically predicted diagonal line. Therefore, it is possible to detect GS with wrinkled structures by choosing a low embedding dimension pair; something which should be helpful in practical applications.

#### IV. CONCLUSION

Noninvertible and wrinkling effects may severely hamper detection of GS by conventional approaches. The detection efficiency can be greatly improved if the pseudofalse effect is reduced. In this paper, we propose the  $\delta^p$ -neighbor method to overcome the noninvertibility effect and the  $\delta^{p,q}$  method

to detect GS with wrinkled structures. We also demonstrated the effectiveness of these approaches by exploring different examples. In fact, it was already mentioned in Ref. [4] that for the noninvertible case, if the history of the drive system is considered, the smeared attractor can be restricted into *smooth* branches. But the method there (which considers the history of the drive as followed through a symbolic dynamics scheme) is only suitable for noninvertible systems with a single positive Lyapunov exponent. The present  $\delta^p$  approach is relatively general and, moreover, for one-dimensional drive systems, gives similar results to the symbolic scheme. We have also shown that the detection of GS for the wrinkled case is somewhat more complicated than the smeared noninvertible case, which is contrary to the conclusions of Ref. [3]. This is because the wrinkled case depends also on the history of the response. We expect these results to be helpful in understanding complicated features regarding the detection of nonlinear synchrony.

#### ACKNOWLEDGMENTS

We are grateful for the support of the James S. McDonnell Foundation. Z.Z. was supported by the NNSF of China, the Special Funds for Major State Basic Research Projects, the Foundation for University Key Teacher by the MOE, the Special Funds for Excellent Doctoral Dissertations, the TRAPOYT in Higher Education Institutions of MOE, and the Huo-Ying-Dong Educational Funds for Excellent Young Teachers.

- 
- [1] A. Pikovsky, M. Rosenblum, and J. Kurths, *Synchronization: A Universal Concept in Nonlinear Sciences* (Cambridge University Press, Cambridge, 2001).
  - [2] C.M. Gray, *Neuron* **24**, 31 (1999); E. Rodriguez *et al.*, *Nature* (London) **397**, 430 (1999).
  - [3] P. So, E. Barreto, K. Josić, E. Sander, and S.J. Schiff, *Phys. Rev. E* **65**, 046225 (2002).
  - [4] V. Afraimovich, A. Cordonet, and N.F. Rulkov, *Phys. Rev. E* **66**, 016208 (2002).
  - [5] B.R. Hunt, E. Ott, and J.A. Yorke, *Phys. Rev. E* **55**, 4029 (1997).
  - [6] L. Kocarev, U. Parlitz, and R. Brown, *Phys. Rev. E* **61**, 3716 (2000).
  - [7] J.C. Chubb, E. Barreto, P. So, and B.J. Gluckman, *Int. J. Bifurcation Chaos Appl. Sci. Eng.* **11**, 2705 (2001).
  - [8] N.F. Rulkov, M.M. Sushchik, and L.S. Tsimring, and H.D.I. Abarbanel, *Phys. Rev. E* **51**, 980 (1995).
  - [9] D.T. Kaplan and L. Glass, *Phys. Rev. Lett.* **68**, 427 (1992); H.D.I. Abarbanel, *Analysis of Observed Chaotic Data* (Springer-Verlag, New York, 1996).
  - [10] Gong Xiaofeng and C.H. Lai, *Phys. Rev. E* **60**, 5463 (1999).
  - [11] H.D.I. Abarbanel, *Analysis of Observed Chaotic Data* (Springer-Verlag, New York, 1996).
  - [12] D.T. Kaplan and L. Glass, *Phys. Rev. Lett.* **68**, 427 (1992).
  - [13] W.L. Ditto, M.L. Spano, H.T. Savage, S.N. Rauseo, J. Heagy, and E. Ott, *Phys. Rev. Lett.* **65**, 533 (1990).